# Rapid Multiwaveband Polarization Variability in the Quasar PKS 0420-014: Optical Emission from the Compact Radio Jet

Francesca D. D'Arcangelo<sup>1</sup>, Alan P. Marscher<sup>1</sup>, Svetlana G. Jorstad<sup>1,2</sup>, Paul S. Smith<sup>3</sup>, Valeri M. Larionov<sup>2</sup>, Vladimir A. Hagen-Thorn<sup>2</sup>, Eugenia N. Kopatskaya<sup>2</sup>, G. Grant Williams<sup>4</sup>, Walter K. Gear<sup>5</sup>

# **ABSTRACT**

An 11-day monitoring campaign in late 2005 reveals clear correlation in polarization between the optical emission and the region of the intensity peak (the "pseudocore") at the upstream end of the jet in 43 GHz Very Long Baseline Array images in the highly variable quasar PKS 0420-014. The electric-vector position angle (EVPA) of the pseudocore rotated by about 80° in four VLBA observations over a period of nine days, matching the trend of the optical EVPA. In addition, the 43 GHz EVPAs agree well with the optical values when we correct the former for Faraday rotation. Fluctuations in the polarization at both wavebands are consistent with the variable emission arising from a standing conical shock wave that compresses magnetically turbulent plasma in the ambient jet. The volume of the variable component is the same at both wavebands, although only  $\sim 20\%$  of the total 43 GHz emission arises from this site. The remainder of the 43 GHz flux density must originate in a separate region with very low polarization. If 0420-014 is a typical case, the nonthermal optical emission from blazars originates primarily in and near the pseudocore rather than closer to the central engine where the flow collimates and accelerates.

Subject headings: galaxies: quasars: general — galaxies: quasars: individual (PKS 0420-014) — physical data and processes: polarization

<sup>&</sup>lt;sup>1</sup>Institute for Astrophysical Research, Boston University, Boston, MA 02215; fdarcang@bu.edu, jorstad@bu.edu, marscher@bu.edu

<sup>&</sup>lt;sup>2</sup>Sobolev Astronomical Institute, St. Petersburg State University, Universitetskij pr. 28, 198504 St. Petersburg, Russia; vml@vl1104.spb.edu, hth@vg3823.spb.edu, kopac@astro.spbu.ru

<sup>&</sup>lt;sup>3</sup>Steward Observatory, The University of Arizona, Tucson, AZ 85721-0065; psmith@as.arizona.edu

 $<sup>^4\</sup>mathrm{Multiple}$  Mirror Telescope Observatory, The University of Arizona, Tucson, AZ 85721-0065; gwilliams@mmto.org

<sup>&</sup>lt;sup>5</sup>School of Physics and Astronomy, Cardiff University, 5 The Parade, Cardiff CF2 3YB, Wales, UK; Walter.Gear@astro.cf.ac.uk

# 1. Introduction

Our knowledge of the jets of active galactic nuclei (AGN) becomes less certain as we consider regions closer to the central engine. However, these regions are the sites of especially interesting physical phenomena, such as acceleration and collimation of the jet flow, formation of the observed "core" of the jet, energization of relativistic electrons, and changes in the geometry of the magnetic field. While it is widely accepted that synchrotron emission is the main mechanism behind continuum production, establishing the location of this emission at different wavebands has been problematic. Imaging with very long baseline interferometry (VLBI) can resolve different components of the jet at radio wavelengths. In addition, variability of the flux density and spectral shape provides information on the small-scale behavior at all wavebands, but the inability to produce high quality images at submilliarc-second resolution at wavelengths shorter than 3 mm allows multiple interpretations that are compatible with the data.

There is, however, an emerging method for establishing the location of the emission at short wavelengths. Similarities of unique polarization signatures of features in both VLBI images and optical measurements provide a possible connection between the two wavebands. Recent work by Gabuzda et al. (2006) and Jorstad et al. (2007), that extend earlier studies by Wardle, Moore, & Angel (1984), Sitko, Schmidt, & Stein (1985), Gabuzda & Sitko (1994), and Lister & Smith (2000), reveals a correlation between VLBI pseudocore (see below) and optical polarization angle in a number of blazars. These results suggest that the two emission regions are either cospatial or separate but with both threaded by magnetic fields having similar geometries. [Here we follow Jones (1988), in referring to the compact feature at the upstream end of the jet in VLBI images as the "pseudocore". This may be an actual stationary feature, such as a standing shock wave (see, e.g., Daly & Marscher 1988; Cawthorne 2006), or the point in the diverging jet flow where the optical depth is of order unity (Blandford & Königl 1979; Königl 1981).]

The most direct way to establish cospatiality of the emission at different wavebands is to observe coordinated variability of polarization that is seen both in the VLBI images and in measurements at shorter wavelengths. In this *Letter* we report observations of polarization variations in both the optical emission and the pseudocore as measured on 43 GHz Very Long Baseline Array (VLBA) images of the quasar PKS 0420–014 (z = 0.915; Hewitt & Burbidge 1993) that span nine days, with no significant time lag. These results place the nonthermal optical emission within the 7 mm pseudocore of the jet.

#### 2. Observations

We collected optical data at two sites. At the Steward Observatory 1.55 m Kuiper telescope, we used the SPOL spectropolarimeter (Schmidt, Stockman, & Smith 1992), making a total of nine measurements from 2005 October 23 to November 3. A 600 lines/mm grating covered an entire diffraction order of  $\sim 400\text{-}800$  nm at a resolution of 1.7 nm. The spectropolarimetry used slit widths of either 2" or 3" along with a 10" spectral extraction aperture. Differential spectrophotometry relative to field stars calibrated by Smith & Balonek (1998) employed a  $5.1'' \times 12''$  (or 14'') aperture. Details of the reduction procedure can be found in, e.g., Smith et al. (2003). We also performed polarimetry and photometry at R band on the AZT-8 70 cm telescope at the Crimean Astrophysical Observatory. The signal-to-noise ratio was low, however, owing to the faintness of 0420-014 (R=17.8-18.3) during the campaign. We therefore do not display the data here, but note that they are consistent with the Steward Observatory results.

We observed 0420-014 at 43 GHz with the VLBA at four epochs during the campaign: October 24, 28 and November 1, 2. After correlation at the Array Operations Center of the National Radio Astronomy Observatory (NRAO) in Socorro, New Mexico, we followed the procedures described in Jorstad et al. (2005) to create and analyze the resultant images. We refer the polarization position angle measurements to a stable feature in the VLBA polarized intensity image of the quasar CTA102. We find good agreement between the adjusted angles of several objects with archival data and with contemporaneous Very Large Array measurements (available on website http://www.vla.nrao.edu/astro/calib/polar/). In our analysis, we add 31° to the polarization angle in the pseudocore of 0420-014 to compensate for Faraday rotation, based on the estimate of rotation measure by Jorstad et al. (2007).

We also observed 0420-014 at two epochs (October 24 and 27) with the Heterodyne Spectrometer at the James Clerk Maxwell Telescope (JCMT) at a frequency of 230 GHz. The sensitivity of the system was sufficient only to determine the flux density of 0420-014 relative to the planets Uranus and Mars.

#### 3. Analysis

On milliarcsecond (mas) scales, the 43 GHz structure of 0420-014 consists of a compact pseudocore and a jet with knots that propagate away from the pseudocore on paths that eventually curve southward (Jorstad et al. 2005). The VLBA images from our campaign (Fig. 1) feature a broad jet extending to 0.7 mas south of the pseudocore. The pseudocore, with a flux density of  $\sim 2$  Jy, has a low degree of polarization, P < 1%, but a highly variable

EVPA (see Fig. 2). The first distinct jet component, a 0.45 Jy knot lying 0.4 mas south of the pseudocore, is more highly polarized ( $P \sim 7\%$ ). Its degree and angle of polarization remained steady throughout the campaign to within the uncertainties (cf. Fig. 2), providing a check on the calibration. The very low polarization of the pseudocore at the third epoch of VLBA data (Julian date 2453675.9) is an artifact of the long observation time ( $\sim 10$  hours) required to obtain a high-quality image. Upon splitting the observation in two, we find that the EVPA varied by  $\sim 90^{\circ}$  from the first half to the second half of the observation, thereby cancelling the polarization in the resultant image shown in Figure 1. The degree of polarization of the pseudocore displayed in Figure 2 for this epoch is the average between the two halves. For the remaining VLBA images, the EVPA did not change by more than  $2\sigma$  between the first and second half of the observation.

The optical polarization underwent pronounced variations in both P and EVPA, as shown in Figure 2. Of particular note is that the 43 GHz pseudocore and optical EVPAs varied in a similar manner, following each other remarkably well over a range of  $\sim 80^{\circ}$ . By eye, we see that a straight line through the three radio points (the polarization of the pseudocore was too weak to measure on November 1) provides a reasonable representation of the overall optical trend. Upon performing a least-squares linear fit to the EVPA vs. time plots that takes into account the uncertainties in the data, we find that the pseudocore polarization vector rotates by  $-10.5^{\circ}\pm0.8^{\circ}$  day<sup>-1</sup>, while the optical vector rotates by  $-11.1^{\circ}\pm$ 0.3° day<sup>-1</sup>. There is no significant time lag between the 43 GHz and optical polarization variations. Despite the similarity in EVPA at the two wavebands, the degree of polarization P is considerably higher ( $\langle P \rangle = 3.0 \pm 0.2\%$ ) at the optical band than in the 7 mm pseudocore  $(\langle P \rangle = 0.47 \pm 0.03\%)$ . This implies that  $\sim 80\%$  of the 43 GHz emission from the pseudocore arises from a separate, essentially unpolarized region that is blended with the pseudocore at the angular resolution of the VLBA. We suggest that this region is optically thick with a tangled magnetic field, in which case the polarization would be very close to zero. A higher resolution 86 GHz polarized intensity image should reveal this component.

# 4. Discussion

The striking correspondence between variations in polarization at the two wavebands locates the primary site of optical nonthermal emission in this quasar within the 7 mm pseudocore. As emphasized by Marscher (2006b), this generally lies well downstream of the central engine and "true core," since the self-absorption turnover frequency of the overall synchrotron spectrum of 0420–014 occurs at a shorter wavelength,  $\sim 3$  mm (Bloom et al. 1994). Our flux density measurements of 2.5 Jy at 7 mm and 1.1 Jy at 1.35 mm dur-

ing the campaign indeed indicate that the turnover was at a wavelength longer than 1.35 mm. The true core might be the end of the bulk acceleration and collimation zone (see Vlahakis & Königl 2004) beyond which the jet is conical with essentially constant mean flow Lorentz factor (Marscher 1980; Jorstad et al. 2007).

Magnetic turbulence is the most straightforward way to explain the low fractional polarization generally observed in the compact jets of quasars at radio wavelengths (e.g., Jones 1988; Hughes 2005). We approximate the turbulence as N cells of equal volume, each with uniform but randomly oriented magnetic field. The randomness dilutes most of the polarization of the source such that the mean degree of polarization  $\langle P \rangle = P_{\text{max}} N^{-1/2}$ , where  $P_{\text{max}} = (\alpha + 1)/(\alpha + 5/3)$  is the maximum linear polarization of incoherent synchrotron radiation and  $\alpha$  is the spectral index of the total flux density spectrum,  $F_{\nu} \propto \nu^{-\alpha}$  (Burn 1966; Jones 1988; Hughes & Miller 1991). The standard deviation about the mean value  $\sigma(P) = 2^{-1/2} \langle P \rangle$ . The mean fractional optical polarization of  $\sim 3\%$  then implies that  $\sim 600$  cells participate in the synchrotron radiation at this waveband.

The polarization of the pseudocore could vary if there were a changeover in turbulent cells involved in the emission during the course of our campaign. This can be accomplished if the radiating electrons are energized by a shock wave that passes through the turbulence (Jones et al. 1985; Jones 1988; Marscher, Gear, & Travis 1992) or vice versa. However, only in the unlikely case of a face-on propagating shock wave would the partial ordering of the magnetic field parallel to the shock front not be apparent from the observer's perspective; otherwise, the compression would affect the polarization by establishing a preferred EVPA (e.g., Hughes & Miller 1991). Furthermore, electrons accelerated at a shock front lose energy as they advect away from the front, with those that attain higher energies—and therefore emit at higher frequencies—having shorter radiative lifetimes. This should cause the optical emission to occupy a much smaller volume ( $\propto \lambda^{1/2}$ ) than does the mm-wave emission (Marscher & Gear 1985), so that the latter should involve  $\sim 60,000$  cells, or  $\sim 100$  times as many as at optical wavelengths. Although this is roughly compatible with the lower mean polarization at 7 mm, it cannot explain the similarity in EVPA in the two wavebands, since the additional factor of  $\sim 100$  cells should produce a mean polarization angle at 7 mm that is essentially independent of the optical EVPA.

In order for a shock plus turbulence model to be valid, the thickness of the section of shocked plasma imposed by gas dynamics (the shocked region ends at a rarefaction; see, e.g., Daly & Marscher 1988; Gómez et al. 1995) must be comparable to the radiative lifetime of the optically emitting electrons times the speed at which the compressed plasma drifts from the acceleration zone at the shock front. The timescale of variability of the optical polarization  $t_{\text{var}} \approx 4$  days (see Fig. 2). If we adopt the apparent speed and angle to

the line of sight of the jet in 0420-014 derived from VLBA monitoring by Jorstad et al. (2005),  $\beta_{\rm app} \approx 11$  and  $\theta \approx 3^{\circ}$  (Doppler factor of 16 and flow Lorentz factor  $\Gamma \approx 11$ ), a section of jet plasma of thickness  $x \sim 0.8$  pc passes by a stationary shock during a time interval of 4 days in the observer's reference frame. The synchrotron radiative lifetime of the electrons at optical wavelengths  $t_{\rm s} \approx 0.18 (B/0.1~{\rm G})^{-3/2}$  yr, where we estimate the magnetic field  $B \sim 0.1$  G by calculating the value corresponding to equipartition between the magnetic and relativistic electron energy densities (see Homan et al. 2006, for evidence that the brightness temperatures of pseudocores of blazars are consistent with equipartition). The energized electrons travel a distance  $\Gamma ct_s \approx 0.6$  pc before they can no longer radiate in the optical band (the  $\Gamma$  factor accounts for Lorentz contraction of the jet length in the plasma frame). This is essentially the same as the value of x estimated above, so that nearly all of the turbulent cells in the emission region are replaced every 4 days, as required by the variability. The length of the section compressed by the shock can be less than the distance traversed by the electrons radiating at optical wavelengths if the shock results from the body pinch-mode instability owing to an oscillating pressure mismatch at the boundary between the jet and the external medium (Daly & Marscher 1988). As seen in numerical gas dynamical simulations (Gómez et al. 1995), such shocks have a conical geometry if the jet is sufficiently close to being circularly symmetric. The partial ordering of the magnetic field owing to compression by a conical shock contributes negligibly to the polarization for very small viewing angles (Cawthorne 2006) such as 3°, the value derived for 0420-014 by Jorstad et al. (2005).

The apparent rotation of the polarization vector can be purely stochastic, as found by Jones et al. (1985), who analyzed a model similar to that described above. We have performed a number of simulations similar to those of Jones et al., incorporating 600 cells, each with the same density and strength of a randomly oriented magnetic field. The simulations produce artificial plots of percent polarization and EVPA vs. time. Rotations by  $100^{\circ}$  or more occur  $\sim 10\%$  of the time. Since 0420-014 was only one of 13 objects observed, the probability of catching one source at the start of a long rotation episode is reasonably high if nearly all blazars behave in a similar manner.

Our observations could also be explained if a feature, e.g., a shock, with a partially ordered magnetic field were to translate down a jet that twists by  $\sim 140^{\circ}$  over the length of  $\sim 9$  pc that the feature would move in 11 days (see, e.g., Gopal-Krishna & Wiita 1992). This is not implausible, since curved jets are common in 43 GHz images of blazars (e.g., Marscher et al. 2002; Jorstad et al. 2005). However, such a model does not naturally explain the variations in degree of polarization and the fluctuations in EVPA about the rotation trend (see Fig. 2). A similar criticism argues against apparent rotation from changing aberration owing to acceleration of a polarized knot as it propagates down the jet (Blandford & Königl

1979). Furthermore, monthly VLBA monitoring throughout 2006 failed to detect any bright knot propagating down the jet that would correspond to a shock wave moving through the pseudocore during our campaign. We can also eliminate a simple two-component model in which two nearly orthogonally polarized regions vary in relative flux density such that the EVPA rotates from that of one feature to that of the other. The maximum rotation possible in such a model is less than 90°, while the optical EVPA changed by considerably more than 100° during the 11 nights of our campaign (see Fig. 2).

# 5. Summary and Conclusions

Our observation of concurrent polarization position angle at optical wavelengths and 7 mm as it swings by  $\sim 80^{\circ}$  over an interval of nine days demonstrates that the main region producing polarized optical emission is the same as that giving rise to the pseudocore at 43 GHz. During this rotation, the degree of polarization varied and the EVPA fluctuated about the mean trend in a manner consistent with a chaotic magnetic field. We propose a model that explains the variations via changeovers in the  $\sim 600$  turbulent cells involved in the emission over a period of a few days. This is accomplished as the plasma advects through a standing, conical shock where electrons are accelerated at the front. The polarized emission at 43 GHz must originate in the same volume as does the optical radiation, a situation that requires the region compressed by the shock to be limited by gas dynamics rather than by radiative energy losses. This agrees with gas dynamical simulations that show alternating regions of conical shocks and rarefactions in jets with circular symmetry (Gómez et al. 1995). We therefore conclude that the 43 GHz pseudocore in 0420-014 corresponds to a standing shock system rather than the site where the optical depth is roughly unity. This is likely to be the case in many blazars, since stationary features near the pseudocore in parsec-scale jets are common (Jorstad et al. 2001).

We are in the process of analyzing data from other objects observed during the campaign as well as objects from a similar campaign in 2006 March-April. These data will determine how frequently rapid, correlated variations in optical and high-frequency radio EVPAs occur in blazars. If this behavior is common, then we can search for similarity in polarization in a number of blazars to identify the locations of optical synchrotron emission on VLBI images. This would allow us to use correlations between optical or mm-wave and X-ray as well as  $\gamma$ -ray variations in total flux density to determine the location(s) of nonthermal emission across a factor of  $\sim 10^{12}$  in frequency (Marscher & Jorstad 2005; Marscher 2006a).

This material is based on work at Boston University supported by the National Science

Foundation under grant AST-0406865, and at St. Petersburg State University supported by grant no. 05-02-17562 from the Russian Fund for Basic Research. P.S.S. acknowledges support from NASA contract 1256424. The VLBA is an instrument of the National Radio Astronomy Observatory, a facility of the National Science Foundation operated under cooperative agreement by Associated Universities, Inc. The JCMT is operated by the Joint Astronomy Centre on behalf of the Particle Physics and Astronomy Research Council of the United Kingdom, the Netherlands Organization for Scientific Research, and the National Research Council of Canada.

#### REFERENCES

Blandford, R. D., & Königl, A. 1979, ApJ, 232, 34

Bloom, S. D., et al. 1994, AJ, 108, 398

Burn, B. J. 1966, MNRAS, 133, 67

Cawthorne, T. V. 2006, MNRAS, 367, 851

Cawthorne, T. V., & Cobb, W. K. 1990, ApJ, 350, 536

Daly, R. A., & Marscher, A. P. 1988, ApJ, 334, 539

Gabuzda, D. C., Rastorgueva, E. A., Smith, P. S., & O'Sullivan, S. P. 2006, MNRAS, 369, 1596

Gabuzda, D. C., & Sitko, M. L. 1994, AJ, 107, 884

Gómez, J. L., Martí, J. M., Marscher, A. P., Ibáñez, J. M., & Marcaide, J. M. 1995, ApJ, 449, L19

Gopal-Krishna, & Wiita, P. J. 1992, A&A, 259, 109

Hewitt, A., & Burbidge, G. 1993, ApJS, 87, 451

Homan, D. C., et al. 2006, ApJ, 642, L115

Hughes, P. A., & Miller, L. 1991, in Beams and Jets in Astrophysics, ed. P. A. Hughes, Cambridge Astrophysics Series, (Cambridge Univ. Press), 1

Hughes, P. A. 2005, ApJ, 621, 635

Jones, T. W. 1988, ApJ, 332, 678

Jones, T. W., et al. 1985, ApJ, 290, 627

Jorstad, S. G., et al. 2001, ApJS, 134, 181

Jorstad, S. G., et al. 2005, AJ, 130, 1418

Jorstad, S. G., et al. 2007, AJ, submitted

Königl, A. 1981, ApJ, 243, 700

Lister, M. L., & Smith, P. S. 2000, ApJ, 541, 66

Marscher, A. P. 1980, ApJ, 235, 386

Marscher, A.P., Jorstad, S.G., Mattox, J.R., & Wehrle, A.E. 2002, ApJ, 577, 85

Marscher, A. P. 2006a, in Blazar Variability Workshop II: Entering the GLAST Era, ed. H. R. Miller et al., ASP Conf. Ser., 350, 155

Marscher, A. P. 2006b, in Relativistic Jets: The Common Physics of AGN, Microquasars and Gamma-Ray Bursts, ed. P.A. Hughes & J.N. Bregman, AIP Conf. Ser., 856, 1

Marscher, A. P., & Gear, W. K. 1985, ApJ, 298, 114

Marscher, A. P., Gear, W. K., & Travis, J. P. 1992, in Variability of Blazars, ed. E. Valtaoja & M. Valtonen, Cambridge U. Press, 85

Marscher, A. P., & Jorstad, S. G. 2005, in Astronomical Polarimetry: Current Status and Future Directions, ed. A. Adamson et al., ASP Conf. Ser., 343, 469

Schmidt, G. D., Stockman, H. S., & Smith, P. S. 1992, ApJ, 398, L57

Sitko, M. L., Schmidt, G. D., & Stein, W. A. 1985, ApJS, 59, 323

Smith, P. S., & Balonek, T. J. 1998, PASP, 110, 1164

Smith, P. S., Schmidt, G. D., Hines, D. C., & Foltz, C. B. 2003, ApJ, 593, 676

Vlahakis, N., & Königl, A. 2004, ApJ, 605, 656

Wardle, J. F. C., & Kronberg, P. P. 1974, ApJ, 194, 249

Wardle, J. F. C., Moore, R. L., & Angel, J. R. P. 1984, ApJ, 279, 93

This preprint was prepared with the AAS IATEX macros v5.2.

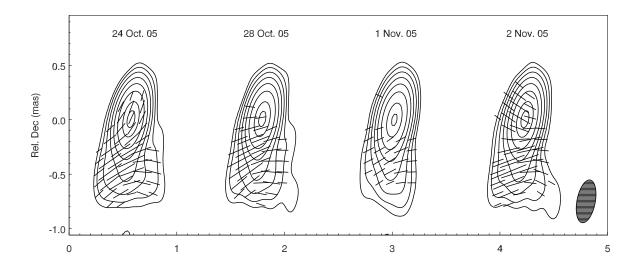


Fig. 1.— 43 GHz (7 mm) images of 0420-014 at the four epochs of VLBA observations. We refer to the region surrounding the peak in total intensity as the "pseudocore." The sacle of the horizontal, right ascension axis, are the same as for the vertical, declination axis. Contours represent 1, 2, 4, 8, 16, 32, 64, and 90% of the peak total intensity of 2.0 Jy/beam, while the sticks indicate polarized intensity (length of 0.1 mas corresponds to 6.2 mJy/beam) and direction of electric vector. Correction for statistical bias and for Faraday rotation toward the pseudocore of  $-31^{\circ}$  at 43 GHz has not been applied to the displayed polarization vectors. As noted in the text, the very low polarization of the pseudocore in the 2005 November 1 image is an artifact of a pronounced change in polarization position angle during the ten-hour observation. The rms polarization noise level is 1.8 mJy/beam. Dimensions of the restoring beam (shown as a shaded ellipse in the lower right corner) are  $0.40 \times 0.17$  mas along position angle  $-11^{\circ}$ .

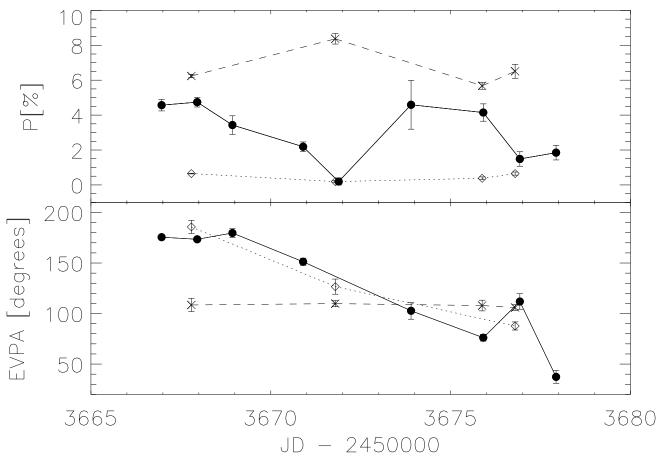


Fig. 2.— Top: Variation of percent polarization with time of 0420–014 in the optical band (450-750 nm; filled circles and solid line), in the 7 mm pseudocore (open diamonds and dotted line), and in the first jet component in the 7 mm image (× and dashed line). The degrees of polarization are corrected for statistical bias (Wardle & Kronberg 1974). Bottom: Variation of EVPA with time of the same three components of PKS 0420–014. The EVPA is not plotted when  $P/\sigma(P) < 1.5$  or for the pseudocore at JD 2453675.9 when it varied greatly during the VLBA observation. A correction of 31° has been added to the EVPAs of the pseudocore to compensate for Faraday rotation. For reference, JD 2453670 is 2005 October 26.